FASE FRONTIERS OF AGRICULTURAL SCIENCE AND ENGINEERING

Engineering Transactions of CAE

RESEARCH ARTICLE

2026 / Volume 13 / Issue 2 / 25651

Piping design and bellows optimization for pneumatic conveying systems based on EDEM-fluent coupled methods for rice

Chengsai FAN[1], Biao CHENG[2], Jiaxin TAN[3], Ruiyin HE (✉)[1], Gaoming XU[4], Jingliu ZHANG[2]

1 College of Engineering, Nanjing Agricultural University, Nanjing 210031, China.
2 Aerosun Corporation, Nanjing 211100, China.
3 Changsha Intelligent Driving Institute, Changsha 410006, China.
4 College of Intelligent Manufacturing and Equipment, Jiangmen Polytechnic, Jiangmen 529090, China.

KEYWORDS

Air distribution, bellows, coupled EDEM-Fluent, design methodology, rice

HIGHLIGHTS

- The influence of structural parameters of bellows on rice in the flow field was analyzed theoretically and verified in simulation experiments.
- Three basic principles for the piping design for a pneumatic seed- discharge system were determined.
- The optimal structural parameters of bellows were obtained through optimization tests.
- The optimal length of the bellow section was determined to be 400−500 mm through extensive bench testing.

Received February 18, 2025;
Accepted June 4, 2025.

Correspondence: ryhe@njau.edu.cn

GRAPHICAL ABSTRACT

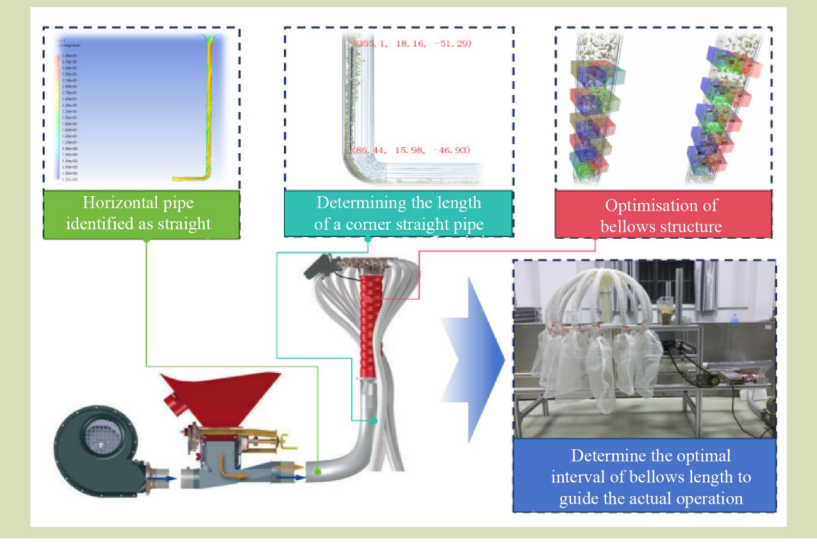

ABSTRACT

Currently, the main optimization of pneumatic conveying seed-discharge systems targets distributors, ignoring the important role of pipelines. In this study, simulations were used to determine an improved structure of the conveying pipe. The horizontal pipe was determined to be a 300 mm straight pipe, which was connected under the vertical bellows as a transition. This study adopted the $L_9(3^4)$ orthogonal test method to optimize the bellows parameters, using as index the coefficient of variation of the uniformity of the bellow outlets. The indoor bench test was designed to validate different flow rate and bellows length combinations. The optimal bellows parameter combination of the corrugated circle had a radius of 8 mm, bellows length of 500 mm, corrugation distance of 40 mm and corrugation length of 16 mm, achieving a 3.46% coefficient of variation of the particle distribution in the

plumbing. Under various particle mass flow rates (33.5, 67.0, 101 g·s^{-1}), the bellows length of the optimal solution was verified to be in the interval of 400–500 mm, and the consistency coefficients of the variations in row displacements of the system satisfied the requirements. This study provides guidance for the design and application of piping in pneumatic seed-discharge systems.

1 Introduction

The pneumatic distribution of seed-discharge systems has been widely promoted because of its small size, high seed-discharge efficiency, and strong adaptability. The pneumatic distribution system, as a high-speed distribution system, has the greatest potential for development. In line with the current development trend of high-speed mechanical operations, it is characterized by high efficiency, cost saving and versatility[1].

An air-blown planter consists of a seed discharger[2], distributor, seed-mixing device and seed-delivery pipe[3]. Yatskul et al.[2,4] studied the effect of various operating parameters on the uniformity of an existing John Deere 1910 planter air-blown seed discharger but did not focus on the mechanism of the effect of the various factors. Existing studies mainly use EDEM and Fluent to compare the distribution diagrams of flow velocity and particles, aiming to investigate the mechanism of the seeder[4–6]. Researchers have conducted experiments on different distributor end-cap shapes[7,8] to obtain a more uniform seed flow. The effects of the duct diameter and length on the airflow field distribution and particle distribution were determined using the discrete element method EDEM-Fluent. The design of seed-mixing devices aimed at minimizing backflow[2] can significantly improve mixing efficiency. Current research focuses primarily on optimizing the venturi components of these devices. Common approaches include three structural configurations: circular cross-section designs[5,6], rectangular cross-sectional implementations, and convex expanding geometries[1,9,10]. Seed delivery pipes are usually designed with transport efficiency and flow stability as the main considerations. However, seed collisions should also be considered to maximize germination rates. For this reason, researchers have considered six combinations of seed-mixing devices and elbow joints[9], and the vortex zone of the elbow joints was determined by Yatskul et al.[2]. However, when arranging a large pneumatic conveyor system, a 90° bend is inevitable[11], thus necessitating the investigation of how to reasonably arrange the pipeline to ensure that the particles in the vertical pipeline distribute uniformly as rapidly as possible.

After entering the bend, the inertial force of the solid particles is non-negligible in a two-phase flow because the fluid is much denser than air[12]. According to the centrifugal sedimentation theory[13], after entering the bend, the particle phase is centrifugally separated from the airflow, that is, the particle-phase shifts outward as a whole to form a particle bundle leaning on the outer side[5,14]. To enhance seed uniformity, the vertical pipe can be structurally designed. The existing pipe structures include straight pipes with smooth inner walls, corrugated bellows, spiral pipes[15], and round protruding bellows. For straight pipes, a higher air velocity requires a length of 1.2 m for the seeds to be uniformly distributed across the cross-section, indicating a longer seed stabilization formation. When the length of the corrugated bellows ranges from 300 to 500 mm, the seeds achieve uniformity. However, tests conducted by Liao et al.[16] showed that more collisions occur inside the pipe. In the case of spiral pipes, seeds have a cyclic distribution across the cross-section and changing the number of distributor seed outlets may affect the row-to-row uniformity. Round-protruding bellows have also been tested[17] and generally have greater uniformity. However, the research on cross-sectional distribution of seeds in round protruding bellows is limited. Currently, research on pipeline designs is insufficient. Therefore, the gas-solid two-phase flow movement should be comprehensively considered. The gas-phase transport efficiency, particle-phase stability and uniformity should be used as indicators when researching the pipeline layout to determine the key design principles. Optimizing the structure of the vertical bellows is crucial. Corrugations or protrusions on vertical bellows can alter the direction of seed movement, which is also a key factor in improving seed uniformity. However, excessive collisions can affect the

uniformity of the rows. Unfortunately, to date, almost no quantitative research has been conducted on corrugated structures.

Therefore, for this study, we focused on the analysis and optimization of the bellows structure and consider the effect of the piping design on the gas-solid two-phase flow. Based on the coupled EDEM-Fluent simulation method, we first determined the structural form of each part of the pneumatic conveying pipe and subsequently optimized the four main structural parameters: corrugation spacing, single corrugation width, corrugation circle radius, and corrugated tube length and further verified the adaptability of the corrugated tube under different operating parameters in indoor bench tests to ensure that the coefficients of variation of the individual rows satisfy the operating requirements.

2 Materials and methods

2.1 Design

2.1.1 Overall structure and working principle

The pneumatic distribution row seed-conveying structure is shown in Fig. 1. The key components include the feed injector, bellows, pneumatic distributor, overall pipeline arrangement and gas source equipment. The working principle is that the fan provides a high-speed airflow to the entire pipeline. When the airflow enters the jet feeder sprayed by the nozzle, the throttling leads to a certain degree of vacuum formation within the mixing type, whereby the material is sucked into the mixing chamber and the gas-solid two-phase flow undergoes preliminary mixing in the conveying pipe. After passing through the bellows, the seed particles are divided into eight parts by the pneumatic distributor, creating eight seed rows in one apparatus.

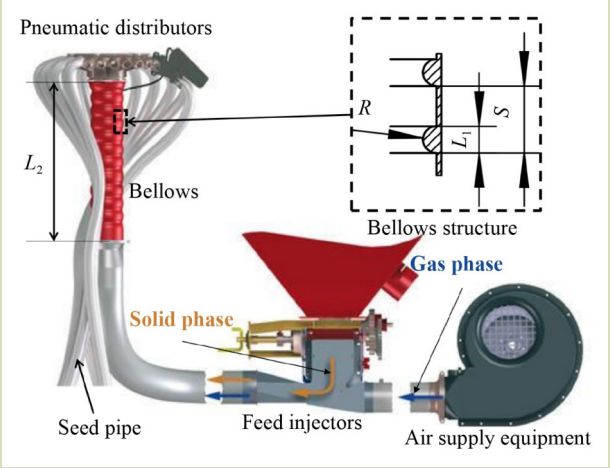

Fig. 1 Pneumatic distribution of seed-discharge conveyor structure and bellows structural parameters. *S*, corrugation spacing; L_1, single corrugation width; *R*, corrugated circle radius; and L_2, bellows length.

Our group predesigned a pneumatic distributor[3] to ensure the consistency of the discharge rows in the case of a uniform distribution of particles and stable velocity of the two-phase flow entering from the main port. The main role of the bellows is two-phase mixing and pipeline center pressurization. In a previous study, rice was uniformly distributed at the end section of the bellows through optimization of the bellow structure.

2.1.2 Commonly used bellows types and bellows variable selection

In the study of pneumatic distribution systems, bellows, also known as pleated pipes, are mostly used. The particles can be distributed more quickly inside the pipe by enhancing the impact of solid particles near the wall and pipe, increasing particle-particle collision, and artificially accelerating the irregular motion of the particle phase. Increasing the folds or corrugations, which corresponds to increasing the coefficient of friction of the pipe wall, increases the wall friction coefficient, which can significantly reduce the particle velocity near the wall, lower the strength of the particle bundles and accelerate their dispersion[18].

Pleated pipes (bellows) were used in this study to improve the uniformity of the distribution of solid particles in the pipe cross-section. The main principle is to consider the gas-solid two-phase flow in the pneumatic distribution process as a homogeneous flow and design a pneumatic distribution system using bellows that serve the functions of pressurization and adequate mixing of the gas-solid two-phase flow[19,20]. However, this study mainly focused on the effect of bellows in the pipeline of the standard distribution system, selecting and calibrating the specific parameters of the bellows on the basis of EDEM-Fluent coupled simulations. From the perspective of pneumatic conveying, the impact of the particle phase inside the pipeline should not result in the reverse movement of

particles; otherwise, excessive pressure loss can occur across the bellows. Therefore, we chose to base the system on circular corrugations, as shown in Fig. 1. The selected bellows variables included corrugation spacing, single corrugation width, corrugated circle radius and bellows length.

2.1.3 Force analysis of seeds in the flow field

Seeds were placed in the airflow field and subjected to the drag force of the airflow. A seed that is not rotating, is subjected to forces, as shown on the left side of Fig. 2(a). When the seed undergoes rotation, it is laterally deflected by the lift force. At this point, the force on the seed is analyzed as follows:

$$F_r + F_s + G = ma_1 \tag{1}$$

$$J\alpha_1 = T_1 \tag{2}$$

$$F_r = \frac{CA_s\rho_g|v_r|v_r}{2} \tag{3}$$

$$F_s = \frac{\pi d_s \rho_g \omega v_r}{8} \tag{4}$$

where, G is the seed gravity (N), F_r is the trailing force of air on seeds (N), F_s is the lift generated by the rotation of a seed (N), T_1 is the total torque on the seed (N·m), ω is the angular velocity of seed rotation (rad·s^{-1}), a_1 is the acceleration of the seeds and α is the angular acceleration of the seed.

Force analysis revealed that the lift force is the main reason for seed dispersion in the straight pipe, but the lift force is small; therefore, the dispersion effect is weak. In fact, after the seeds flow through the bend, they are mainly distributed on the outside of the pipe because of inertia. The straight pipe cannot disperse the seeds effectively, and hence the seeds are not uniformly distributed within the cross-section, which makes it difficult for the seeds to uniformly distribute after being dispensed to each row. We refer to this almost collision-free case as Case 1. However, in addition to the above motion processes in the bellows, additional collisions can occur with bellow protrusions and direction changes because of the turbulence in the airflow. The movement of the seed colliding with the bellows protrusion was analyzed. The force analysis at the moment of collision is shown in Fig. 2(c).

$$F_r + F_s + G + F_p = ma_2 \tag{5}$$

$$J\alpha_2 = T_2 \tag{6}$$

where, F_p is the reaction force of the collision between the seed and closure, which is expressed as $F_p = m\Delta v/\Delta t$, according to the momentum principle (N), T_2 is the torque applied to the seed, which contains the torque generated by a combination of friction and Magnus forces as well as airflow.

During this collision, the motion of the seed at the next moment is related to F_r, F_s, G and F_p. According to the

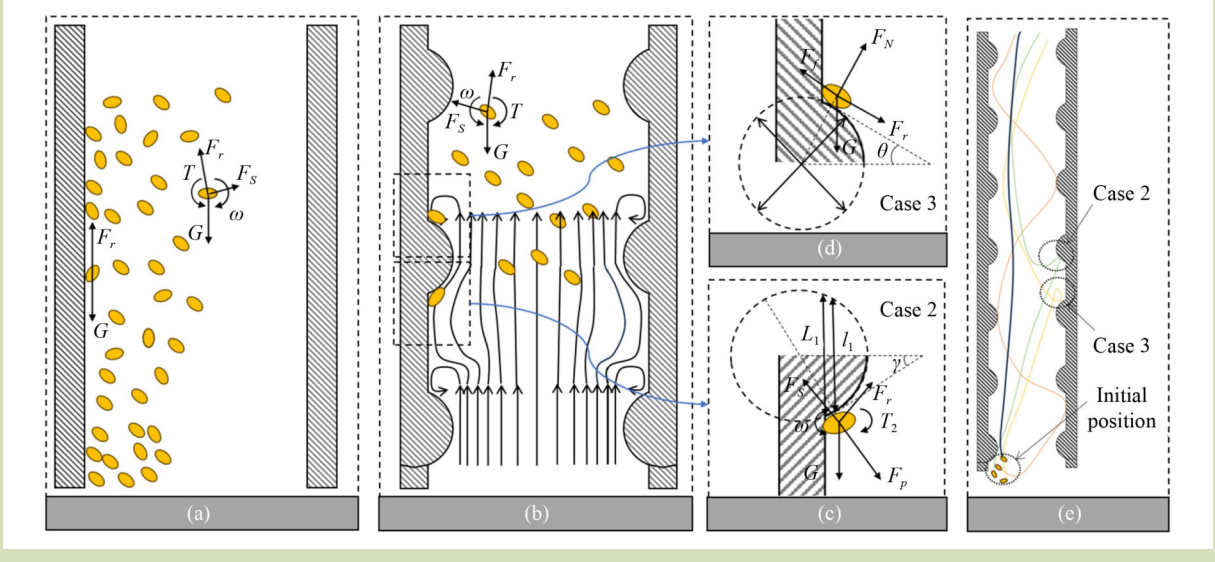

Fig. 2 Force analysis of seeds in the flow field. (a) Force analysis of rice in straight tube, (b) force analysis of rice in bellows, (c) Case 2 force analysis, (d) Case 3 force analysis, and (e) schematic diagram of the trajectory of the rice in the bellows.

momentum theorem, F_p has a decisive effect in the collision process and its direction can be determined. The angle with the horizontal direction is γ, which through a geometric relationship is determined as $\gamma = \arccos l_1/2R$, where l_1 and L_1 are directly related. Therefore, the direction of F_p is related to the structural parameters of the bellows L_1 and R. Consequently, the direction of motion of the seed at the next moment is affected by L_1 and R. We refer to this case as collision Case 2.

The special case (Case 3) in the bellows refers to a special phenomenon caused by the presence of a Kamen vortex street. The air travels back after passing through the obstacle, and this backflow may allow the seeds to stay briefly above the bellows protrusion. The force analysis is shown in Fig. 2(d) (analyzing the equation is beyond the scope of this paper). The larger the bellows protrusion is, the larger is the vortex, and the seed is more likely to dwell on the protrusion. Excessive dwell time may affect the seed flow stability. The structural parameters S and L_2 affect the frequency of occurrence in Case 3 and hence the homogeneity of seeds across rows.

A theoretical analysis of the trajectory of the seeds moving in the bellows is shown in Fig. 2(d). Due to inertial forces, the seeds almost always start from outside the bellows. Seeds may exist in the presence of Case1 (blue trajectory line) and in Case 2 at a certain moment (rosy red trajectory line). Seeds are also affected by Case 3 (green trajectory line) and there are also seed particles that may have multiple collisions (orange trajectory line). All trajectory lines show that frequent random collisions and vortex perturbations are responsible for the significant improvement in the uniformity of particle distribution in the cross-section, reflecting a dual mechanism of collision dissipation-vortex perturbation in the bellows.

2.2 Discrete element-coupled computational fluid dynamics simulation approach

2.2.1 Mathematical modeling using a computational fluid dynamics-discrete element method

The effect of the particles on the gas flow field is negligible in this problem because of their limited gas occupancy and small particle size[21,22]. In the EDEM simulations, a procedure is used to track the motion and collisions of particles during the distribution process. Particle motion is governed by Newton's second law of motion, and the equations[6] for translational and rotational motion are:

$$m_i \frac{\mathrm{d}v_{p,i}}{\mathrm{d}t} = F_{pf,i} + \sum_{j=1}^{n_i} (F_{n,ij} + F_{t,ij}) + F_{w,i} + m_i g \tag{7}$$

$$I_i \frac{\mathrm{d}\omega_{p,i}}{\mathrm{d}t} = \sum_{j=1}^{n_i} (T_{t,ij} + T_{r,ij}) + T_{w,i} \tag{8}$$

where, m_i is the particle mass (kg), $v_{p,i}$ is the particle velocity (m·s^{-1}), $F_{pf,i}$ is the particle-fluid interaction force, including drag force, buoyancy, Saffman lift force and Magnus lift force (N), $F_{w,i}$ is the contact force between wall and particle (N), $T_{w,i}$ is the torque between wall and particle (N·s^{-1}), g is acceleration due to gravity (m·s^{-2}), I_i is the moment of inertia of the particle (kg·m^{-2}) and $\omega_{p,i}$ is the particle rotation velocity (rad·s^{-1}). Interparticle forces include the normal force $F_{n,ij}$ and tangential force $F_{t,ij}$ (N). The torques acting on particle i by particle j include the tangential torque $T_{t,ij}$ and rolling friction torque $T_{r,ij}$, N·s^{-1}.

The gas phase was assumed to be continuous, obeying the laws of conservation of mass and momentum. The governing equations[6] are expressed as:

$$\frac{\partial(\varepsilon_g \rho_g)}{\partial t} + \nabla \cdot (\varepsilon_g \rho_g v_g) = 0 \tag{9}$$

$$\frac{\partial(\varepsilon_g \rho_g v_g)}{\partial t} + \nabla \cdot (\varepsilon_g \rho_g v_g v_g) = -\varepsilon_g \nabla p + \nabla \cdot (\varepsilon_g \tau_g) + \varepsilon_g \rho_g g - F_{p-g} \tag{10}$$

where, t is the time (s), ρ_g is the air density (kg·m^{-3}), ε_g is the void fraction, v_g is velocity of gas (m·s^{-1}), τ_g is fluid viscous stress tensor (Pa) and F_{p-g} is the source term for the momentum exchange between particles and fluid (kg·m^{-2}·s^{-2}).

2.2.2 Rice basic parameters

The pneumatic distribution seed-discharge system was designed to discharge seeds of rice, particularly cultivar Southern Japonica 9108, as shown in Fig. 3(b). This is a more compact plant type, displaying more vigorous growth, stronger tillering force, stronger resistance to collapse and a late ripening phase, among other advantages. The measured rice-related parameters are listed in Table 1.

The maximum delivery capacity of the distribution system was determined to be 180 g·s^{-1}. The solid-gas mixing ratio of 2.5 was selected based on predetermined parameters: particle suspension velocity of 9.94 m·s^{-1}, particle group suspension velocity of 9.87 m·s^{-1}, conveying air velocity of 26 m·s^{-1} and conveying pipeline diameter of 55 mm.

Table 1 Rice-related parameters

Parameters	Value
True density (g·cm^{-3})	1.1241
Bulk density (g·cm^{-3})	0.5858
Thousand grain weight (g)	28.0498
Equivalent ball diameter (mm)	3.9199
Sphericity (%)	51.585
Particle three-dimensional size parameters (mm^3)	7.621 × 23.410 × 2.332

2.2.3 Simulation modeling

As shown in Fig. 3, the horizontal-vertical 90° bend model and different models of bellows were established using Creo software. The internal cavity of the pipe was filled using the ANSYS design modeler[23], and cavity meshing was generated using ANSYS-Meshing. The experimental particles had an overall ellipsoidal shape, with average length, width and height of the three axes as 7.62, 3.41 and 2.33 mm, respectively calculated assuming spherical particles based on the principles of the EDEM software[24]. This study adopted the method of stacking spherical particles to solid particles for modeling, as shown in Fig. 3(b). The mesh model had to be checked and mesh quality reporting was required before setting the Fluent parameters, as shown in Fig. 3(e).

2.2.4 EDEM parameter determination

In this study, EDEM 2018 was used. The Hertz-Mindlin (no-slip) model combines Hertz's nonlinear elastic collision theory and Mindlin's tangential friction theory to accurately describe the normal elastic contact force and tangential friction behavior between particles. The model assumes no relative sliding between the particles and contact surface, which simplifies the computational complexity, making it suitable for the dry and low-adhesion physical properties of rice seeds. Therefore, the Hertz-Mindlin (no-slip) collision contact model was used for intra-particles and between particles and walls[6,11]. Particle generation location was randomly distributed. The particle factory was set to dynamically generate particles, and maximum particle mass flow rate was 6420 particles s^{-1}. The specific settings are listed in Table 2. As the main discussion here focuses on the influence of the bellows parameters on particle beam dispersion, the larger the mass flow rate of the particle beam, the more difficult it is for it to disperse. Therefore, the maximum particle mass flow rate was used in the simulation test, that is, the particle creation rate was 6420 particles s^{-1}. The specific settings are listed in Table 2.

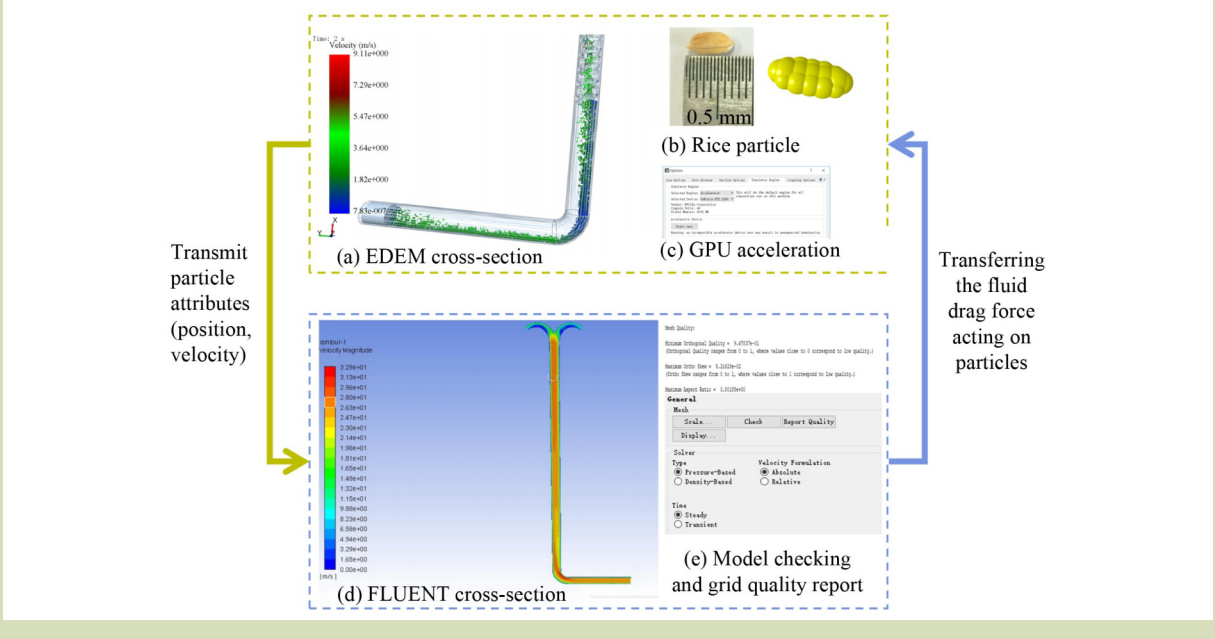

Fig. 3 EDEM-fluent coupling simulation environment construction.

Table 2 EDEM parameter settings

Item	Parameter	Numerical value	Notation	Unit of measure
Solid particle parameters	Poisson's ratio	0.3[a]	ν_s	(–)
	Density	1124[a]	ρ_s	kg·m^{-3}
	Shear modulus	2.6 x 10^8 [a]	G_p	Pa
	Maximum mass flow rate	180.0539[a]	G_s	g·s^{-1}
Equipment materials (engineering plastics)	Poisson's ratio	0.5[a]	ν_e	(–)
	Density	900[a]	ρ_e	kg·m^{-3}
	Shear modulus	1 × 10^8 [a]	G_e	Pa
Interparticle	Restitution coefficient	0.55[b]	e_{pp}	(–)
	Coefficient of static friction	0.56[b]	μ_{spp}	(–)
	Coefficient of rolling friction	0.01[b]	μ_{rpp}	(–)
Between particles and equipment	Restitution coefficient	0.5[b]	e_{pe}	(–)
	Coefficient of static friction	0.45[b]	μ_{spe}	(–)
	Coefficient of rolling friction	0.15[b]	μ_{rpe}	(–)
Gas phase	Entrance speed	26[a]	v_a	m·s^{-1}

Note: [a] Measured values; and [b] sourced values[25] that were further calibrated.

2.2.5 Fluent parameter determination

Fluent software (version 17.0) was used in this study. The main settings required in Fluent are the coupling file loading, model selection, algorithm selection, and inlet and outlet boundary conditions. In this study, we adopted *k*-ε and a realizable model. The particle phase was provided by EDEM, without any need for additional settings after selecting EDEM-Coupling. The inlet velocity conditions were a wind speed of 26 m·s^{-1}, the direction was perpendicular to the inlet plane, the hydrodynamic diameter was set, and turbulence intensity of the fluid was calculated using the following equation.

$$I = 0.16Re^{\left(-\frac{1}{8}\right)} \tag{11}$$

where, *Re* is the Reynolds number.

The hydraulic diameter of the circular pipe was equal to its diameter. Therefore, the turbulence intensity was set to 3.7%, and the hydraulic diameter was 0.055 m. The particle discharge outlet was set as the zero-pressure outlet boundary condition, and a stationary boundary condition was adopted for the wall surface. The SIMPLEC algorithm was used, and the Fluent time step was set to 100 times the EDEM time step.

2.3 Simulation test environment

To calculate the coefficient of variation of the rice distribution uniformity in the virtual test, a grid box group was set up at the outlet of the bellows in the upward portion every 30 mm, thereby dividing into four grid boxes with the center of the pipeline as the reference and box height of 20 mm (Fig. 4). In observing the output window of the simulation file, the two-

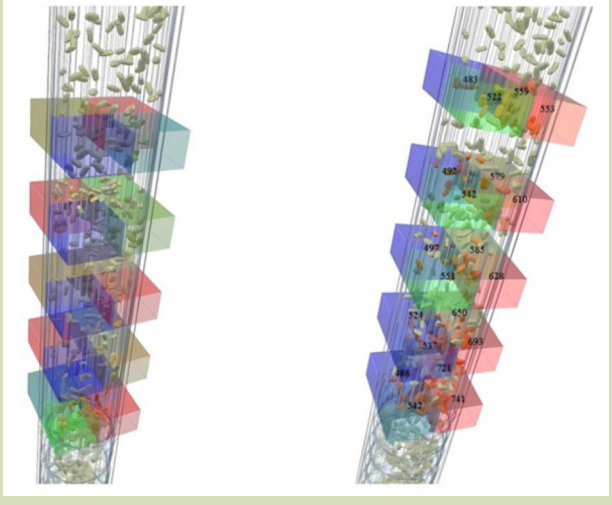

Fig. 4 Delineation of grid boxes and counting the number of particles in each box.

phase flow starts to stabilize as a whole at t of 0.98 s, starting at t of 1.2 s and ending at t of 2.0 s. The number of particles passing through each box during this period was counted statistically, to determine the coefficients of variation between each box in each layer of box groups, which were averaged to determine the distribution of particles in the pipeline in the five layers.

2.4 Indoor bench test

The bench experiments systematically evaluated the performance of the bellows to identify the simulation-optimized design parameters. The main problem is making the distribution effect more uniform. Therefore, a test was conducted to verify the uniformity of the distribution effect at the end, and the specific index of the uniformity coefficient was analyzed against the control group of the straight tube. The specific index was the coefficient of variation of the uniformity of each displacement row.

The purpose of the indoor bench test was to determine the optimal parametric solution of the bellows obtained from the simulations. The distributor had a circular 16-row design with delivery outlets evenly distributed within the circle. The design principle of this distributor was to minimize the excess collisions of particles in the distributor lumen. If the particle flow into the distributor is evenly distributed within the tube, a better distribution effect is obtained. The equipment used for the test is listed in Table 3, and the test rig is shown in Fig. 5.

2.5 Test indicators

The main evaluation metric for the indoor test was the uniformity coefficient of variation. The statistical method of the coefficient of variation of uniformity refers to GB/T 25418-2010[25]. The number of statistical sowing rows was not less than six, and eight rows were counted in this study. The standard deviation (S) and coefficient of variation (V) of the consistency of the flow rate distribution between the rows were calculated as:

$$\overline{X} = \frac{\sum_1^n X}{n} \tag{12}$$

$$S = \sqrt{\frac{\sum (X - \overline{X})^2}{n-1}} \tag{13}$$

$$V = \frac{S}{\overline{X}} \times 100\% \tag{14}$$

$$\overline{V} = \frac{\sum_1^i V}{i} \times 100\% \tag{15}$$

where, X is the mass per row in the bench test and indicates the cumulative mass of rice passing through each box in the simulation experiment, the number of samples was eight in the bench test (interlace selection) and four in the simulation experiment, as in Fig. 4, $\overline{V}$ is the coefficient of variation of the simulation experiment (%), i is the number of boxes used for statistics in the simulation experiment, and the number of boxes in this study was five, as shown in Fig. 4.

3 Results and discussion

3.1 Feasibility analysis of horizontal bellows based on Fluent simulation

When air flows through the bend, significant velocity fluctuations occur near the inner and outer walls. Through numerical simulations of single-phase flows in pipelines with

Table 3 Experimental material model

Device name	Model number	Accurate	Supplier
Anemometer	GM8903	0.001 m·s^{-1}	Shenzhen Jumoyuan Technology Co.
Electronic balance	20002	0.01 g	Hangzhou Youheng Weighing Equipment Co.
Dial calipers	91511	0.03 mm	Seda Tools Co.
Centrifugal fan	HG-2200		Zhejiang Yashba Motor Co.
Converter	SKIV600A2D2G-2	0.01 Hz	Hangzhou Sanke Frequency Conversion Technology Co.
Performance test bench	Self-restraint	(–)	(–)
Key components of air distribution system	Self-restraint	(–)	(–)

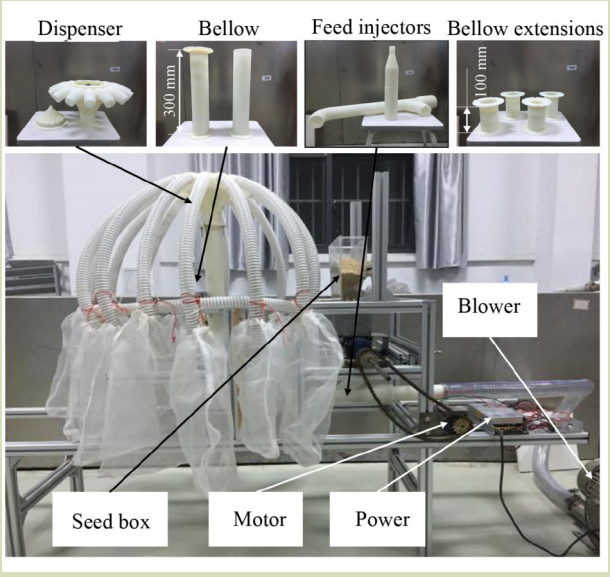

Fig. 5 Test bench.

90° horizontal-to-vertical bends, the flow stabilization length of the airflow, that is, the distance required for airflow with intense fluctuations to regain stability, can be determined. Usually, airflow stability is considered an indicator of particle stabilization[14,17]. In this section, we report experiments designed to observe the flow-field distribution under different duct types. The height of the vertical pipe was set to 1.6 m to observe the flow stabilization process in the vertical pipe. For this purpose, we designed four simulation scenarios, as listed in Table 4.

The numerical simulation results reveal significant airflow velocity discrepancies near the pipe elbow. When the flow path length is insufficient, the velocity distribution within the circular cross-section has pronounced non-uniformity. As the airflow travels further along the vertical pipe segment, the velocity profile gradually stabilizes, achieving improved uniformity. Specifically, longer vertical pipe lengths correspond to more homogeneous velocity distribution patterns in contour plots.

Table 4 Test arrangement

Test No.	Vertical pipe	Horizontal pipe
1	Straight pipe	Straight pipe
2	bellows	Straight pipe
3	Straight pipe	bellows
4	bellows	bellows

Comparative analyses between Tests 1 and 2 (Fig. 6(a,b)) revealed two critical phenomena. The homogenized flow velocity at the pipe centerline increased from baseline values to 28–33 m·s^{-1}, accompanied by progressive amplification of the velocity gradient between wall boundaries and central regions. Flow stabilized within the vertical pipe segment at 1.0–1.2 m, indicating that under current pipeline configuration constraints, the required minimum stabilization length of 1.0 m must be maintained to achieve quasi-steady flow conditions after elbow-induced flow disturbances.

The comparative analyses between Tests 2 and 4 (Fig. 6(b,d)) demonstrated that following an increase in horizontal central airflow velocity, the flow stabilization length within vertical bellows has a marked elevation. Also, a cross-examination of all four experimental configurations revealed that horizontally corrugated piping systems amplify the central airflow velocities, concurrently inducing prolonged flow stabilization requirements in the vertical segments.

These findings support the preferential adoption of smooth-walled horizontal straight pipes in conveying system designs to minimize energy penalties and flow instability risks.

3.2 Analysis of bellows installation position based on EDEM-Fluent coupled simulation

During the simulation test, the motion state of the seed particles in the horizontal pipe is shown in Fig. 7(b) for an air flow velocity of 26 m·s^{-1}. Given that the density of rice is relatively high compared to that of air, the seeds move close to the lower half of the horizontal pipe. The seed flow in the bent pipe is shown in Fig. 7(a). The particle phase undergoing centrifugal separation moves close to outside the bent pipe. At this time, the plumbing pipe in the bellows arrangement is too close to the bend, and seed particles produced by corrugation blocking lead to accumulation of seed particles in the bend, as in Fig. 7(c), which in turn leads to a reduction in the flow rate in the horizontal pipe. In the front section of the horizontal pipe, the acceleration acquired by the rice seed particles is not sufficient, easily leading to the cutoff phenomenon observed in Fig. 7(d).

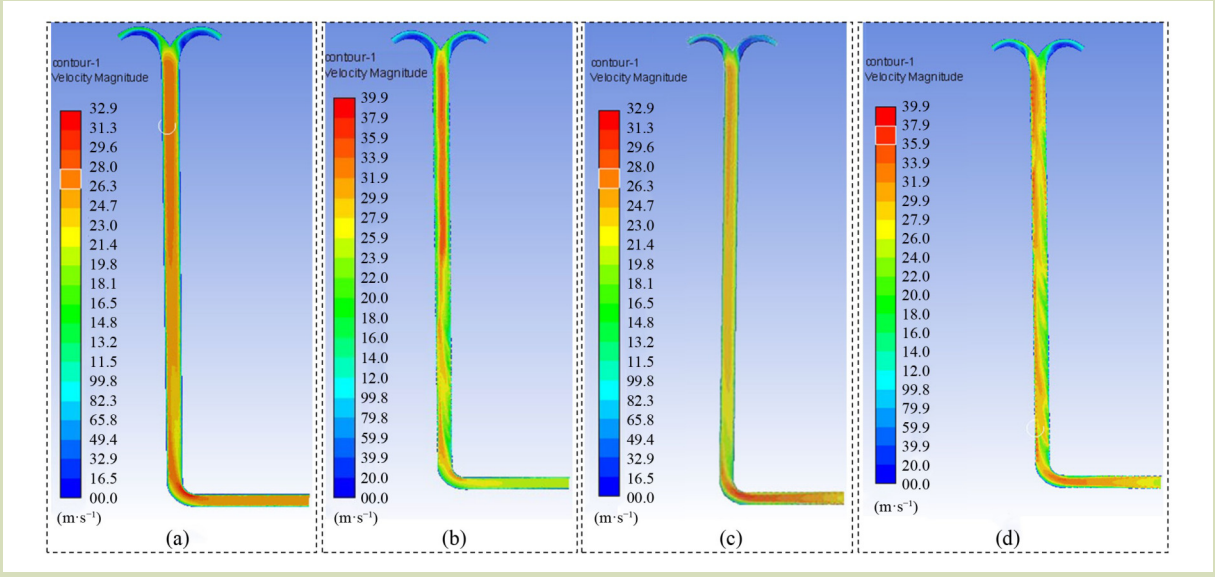

Fig. 6 Based on Fluent simulation test results. (a) Test 1 cloud map of airflow velocity, (b) Test 2 cloud map of airflow velocity distribution, (c) Test 3 cloud map of airflow velocity distribution, and (d) Test 4 cloud map of airflow velocity distribution.

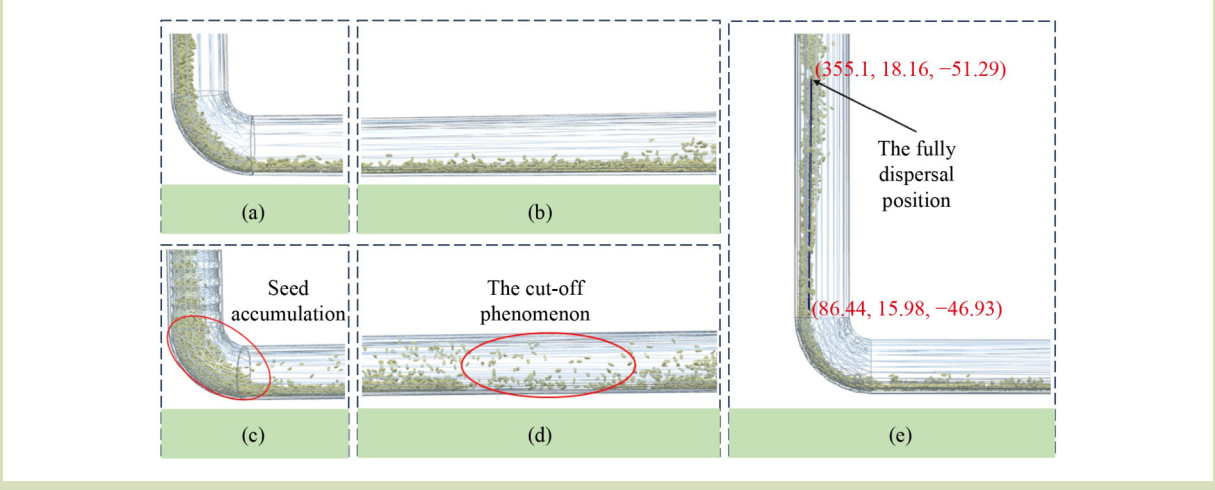

Fig. 7 Based on Fluent-EDEM coupled simulation test results. (a) Motion of seed particles in elbows, (b) movement of seed particles in horizontal tubes, (c) seed particle accumulation caused by too close distance between elbow and bellows, (d) cutoff phenomenon of seed particle flow, and (e) simulation effect of lead vertical tube.

In the simulation of the plumb pipe, the seed particles tend to disperse at a certain distance after passing through the pipe elbow. Therefore, the arrangement of the bellows was assumed to be on the back side of the position where the particle beam had a tendency to disperse, to eliminate the accumulation of seed particles at the bend. The simulation effect of the plumb pipe is shown in Fig. 7(e).

After the basic stabilization of the tube flow, five moments were randomly selected from the simulations: t of 0.9, 1.25, 1.6,

1.95 and 2.3 s. The maximum value of the distance between the fully dispersal position of the seed particles and mouth of the bent tube in these five moments was used as a reference for the required increase of the straight tube. The length measurement was made using the Ruler tool that comes with EDEM. These data are presented in Table 5.

The bellows should be arranged as far back as possible to satisfy all the circumstances. Therefore, the length of the straight pipe was selected to be 300 mm, that is, from the middle of the bent pipe bellows, a distance of 300 mm is added to the straight pipe. No further ripples were found to impede the seed flow during subsequent tests.

3.3 Particle motion analysis in bellows based on coupled EDEM-Fluent simulation

In this section, the mechanism of bellows on the uniformity of rice seed distribution is systematically analyzed using EDEM, comparing the particle movement patterns in straight and corrugated tubes. Parameter combinations of 30 mm corrugation spacing, 14 mm corrugation length of 10 mm corrugation circle radius, and 400 mm tube length were selected for the bellows. In the straight pipe, the particles exhibited an evident left-sided enrichment phenomenon after bending. The cross-sectional diagram shows that although some particles show a tendency to move to the right, they are unable to break through the inertial force bounding of the flow field within the limited pipe length, resulting in very little improvement in cross-sectional uniformity, as shown in Fig. 8.

Compared with the unidirectional flow field of the straight tube, the bellows reconstructs the particle trajectory through the raised structure. As shown in Fig. 9(a), the particle flow undergoes a significant rightward deviation at the first corrugated bump, followed by several collisions to form an oscillatory attenuation motion, which ultimately significantly improves the cross-sectional homogeneity. This dynamic equilibrium results from the synergistic effect of three types of

Table 5 Time-start divergence location table

Item	Value				
Time (s)	0.9	1.25	1.6	1.95	2.3
Length (mm)	289	300	284	222	286

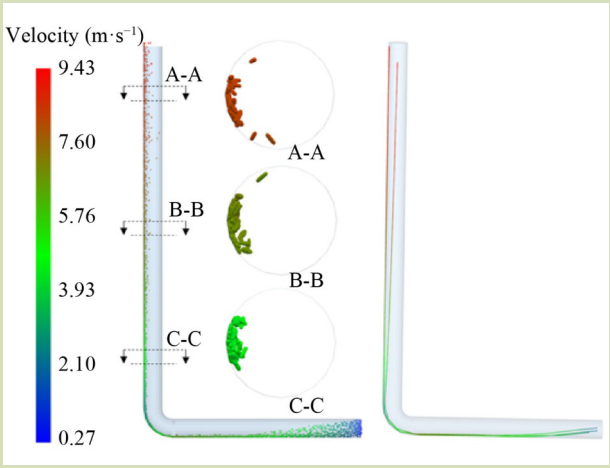

Fig. 8 Motion of particles in a straight tube.

typical motion modes: the particles collide directly with the bumps, resulting in an abrupt change in the velocity direction (Case 3); the particles are pulled by the vortex above the bumps, resulting in velocity decay and secondary deflection (Case 2); and the particles maintain their motion inertia along the central high-speed channel (Case 1). Particle trajectory tracking shows that the trajectories of particles at almost the same location diverge to different locations after collision, confirming the theoretical hypothesis that random collisions significantly improve the cross-sectional uniformity of particles.

To illustrate the collision of seeds inside bellows using quantitative data, we established two groups inside the EDEM. The masses of the y-direction velocities (vertically upward is positive), and masses of the particles in the groups are shown in Fig. 9(c). The average velocity of Group 2 particles is around 9 $m \cdot s^{-1}$, which is about twice the velocity of Group 1 particles (4.5 $m \cdot s^{-1}$) although the former mass (5 g) is significantly higher than that of the latter (2 g). This indicates that a large number of particles collide in the bellows, causing the velocity to decrease or increase, which corresponds to the results of the intuitive analysis. Less mass fluctuation was observed in Group 2 particles, which favors longitudinal uniformity of rice sowing.

Combining the flow-field visualization and quantitative data, the bellows have a significant effect on rice uniformity, which verifies the dual action mechanism of vortex perturbation-collision dissipation in the theoretical model. Therefore,

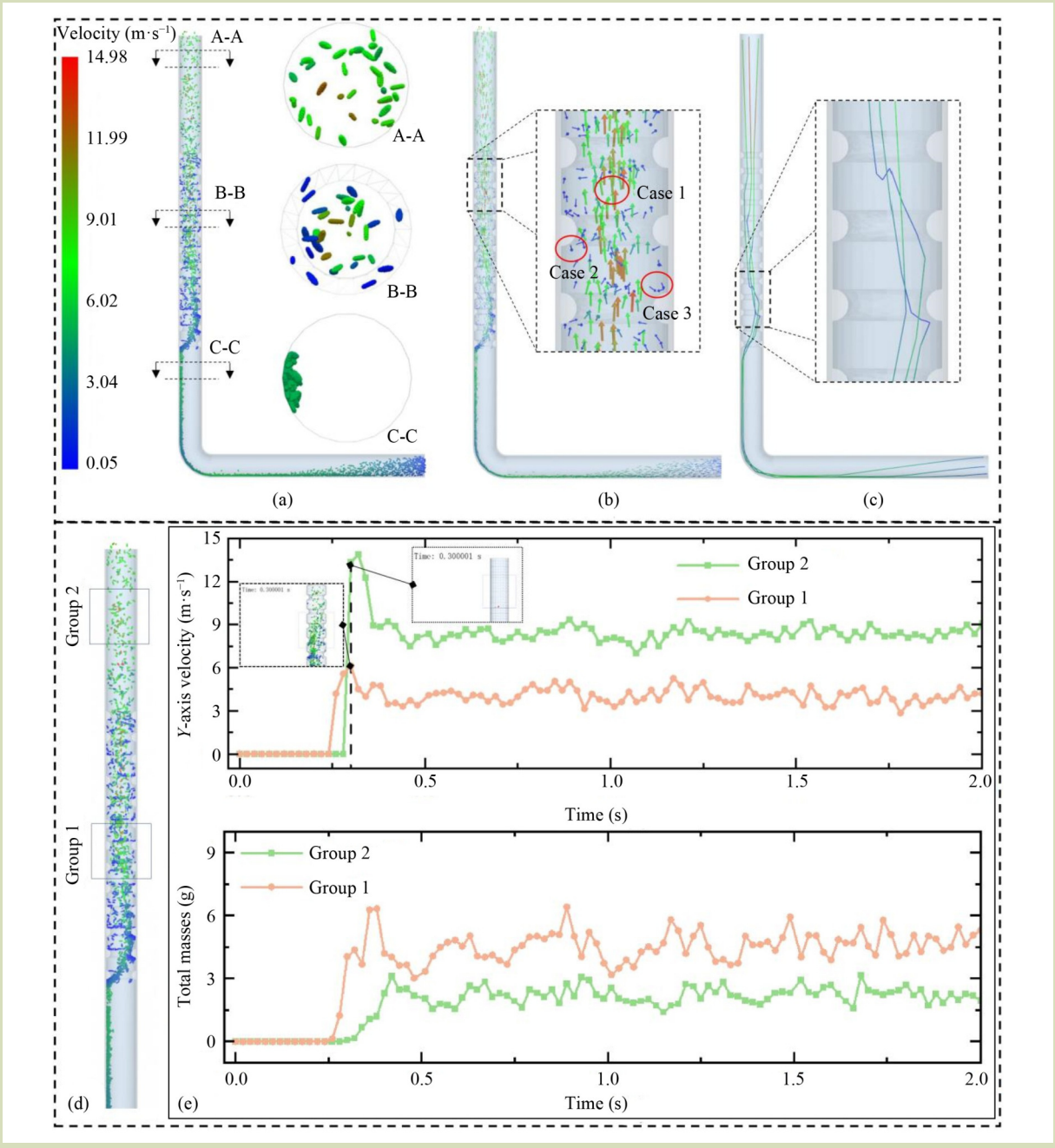

Fig. 9 Particle distribution inside the bellows. (a) Particle distribution at different cross-sections within the vertical pipe, (b) velocity vector diagram of particles in the corrugated pipe section, (c) trajectories of selected particles within the pipe, (d) schematic diagram illustrating the locations of Group 1 and Group 2, and (e) Y-axis velocity and mass statistics for Group 1 and Group 2.

optimization tests can be designed to determine the optimal parameter combinations of the corrugation distance, corrugation length, radius of the corrugated circle and bellows length.

3.4 Optimization results based on EDEM-Fluent coupled simulation

The EDEM-Fluent coupled simulation was used for the optimization of the bellows, with selected bellows variables

including corrugation distance (20–40 mm), ripple length (12–16 mm), radius of the corrugated circle (8–12 mm) and bellows length (300–500 mm). Each variable was determined at three levels. The optimization test method was the $L_9(3^4)$ orthogonal test. The principle of orthogonal test is to rationally arrange the experimental combination of multi-factors and multi-levels through the use of an orthogonal table to ensure that the different levels of each factor are uniformly distributed and independent of each other in the test, to efficiently analyze the effect of each factor on the results using a minimum number of tests. The results of the experimental design are listed in Table 6. Coefficient of variation of the rice distribution uniformity was used as an evaluation index.

Data from the simulation test and results of the polar analysis are listed in Table 5. The major factors were determined based on the polarities:

$$C > D > A > B$$

Based on an analysis of the experimental results (Table 6), among the currently set levels of factors, the most homogeneous scheme for the dispersion of particles in the tube were: corrugated circle radius of 8 mm, bellows length of 500 mm, corrugation distance of 40 mm and corrugation length of 16 mm. The homogeneity increases significantly with an increase in the length of the corrugated tube and according to the factor-indicator diagram (Fig. 10), the gas-solid two-phase pipe flow tends to become more homogeneous as the bellows length increases.

EDEM-fluent coupled simulation experiments were performed using this optimal scheme, and the test index for particle homogeneity in the tube was 3.46%.

3.5 Indoor bench test design

From the EDEM-Fluent coupled simulation test, the difference in the coefficient of variation of the particle distribution in the tube between the tests with and without bellows reached up to

Table 6 Analysis of test data and calculations

Test No.	Level of factors				Test indicators
	Corrugation distance (mm)	Corrugation length (mm)	Radius of corrugated circle (mm)	Bellows length (mm)	Coefficient of variation of particle distribution in the tube (%)
1	20	12	8	500	4.03
2	20	14	10	400	5.89
3	20	16	12	300	10.35
4	30	12	10	300	8.51
5	30	14	12	500	8.97
6	30	16	8	400	5.48
7	40	12	12	400	10.09
8	40	14	8	300	5.89
9	40	16	10	500	4.09
K_1	20.267	22.632	15.397	17.088	
K_2	22.959	20.750	18.490	21.4600	
K_3	20.076	19.920	29.415	24.754	
k_1	6.756	7.544	5.132	5.696	
k_2	7.653	6.917	6.163	7.153	
k_3	6.692	6.640	9.805	8.252	
R	0.961	0.904	4.673	2.556	
Best level	A_3	B_3	C_1	D_1	
CK	Pure straight pipe (measurement start position at 800 mm of straight pipe length)				22.82

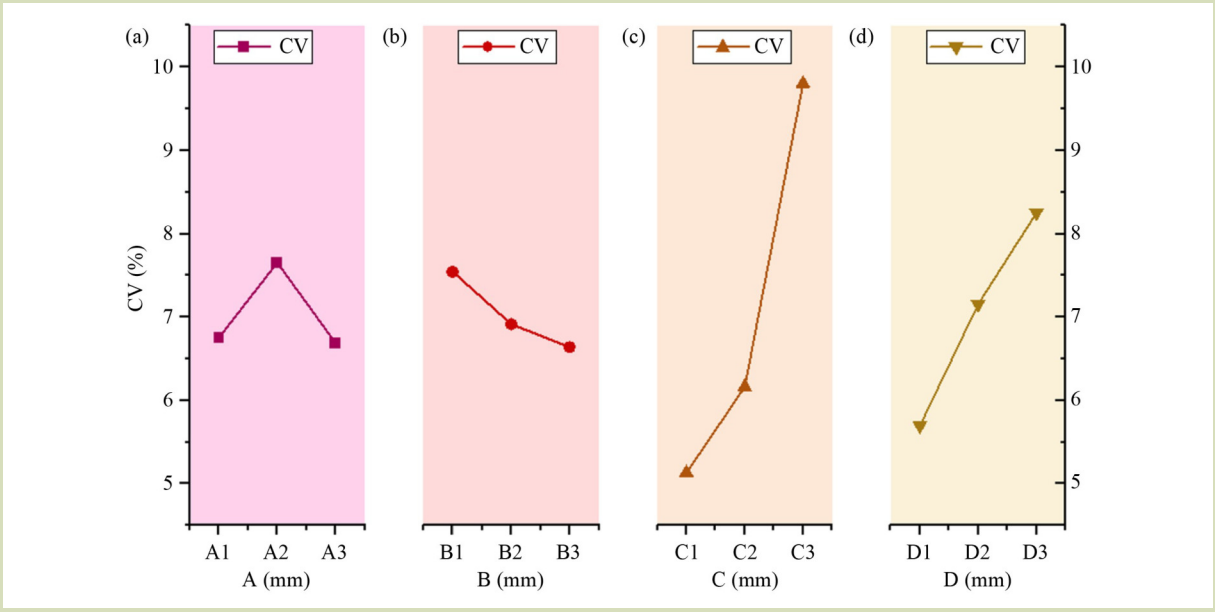

Fig. 10 Factor-indicator map. (a) The effect of corrugation distance on the coefficient of variation, (b) the effect of corrugation length on the coefficient of variation, (c) the effect of radius of corrugated circle on the coefficient of variation, and (d) the effect of bellows length on the coefficient of variation.

18.7781%, which means that the bellows are crucial for the dispersion of particles in the tube. From the factor-indicator diagram (Fig. 10), the change in bellows length can likely lead to a change in uniformity. In the actual installation process, the length of the bellows often depends on the actual installation position; therefore, under the condition that the other factors are at their optimal levels, a one-way test was conducted to analyze the length of the bellows (validation test of the optimal parameter was also included in this one-way test) to explore the optimal length interval of the bellows under different operating conditions.

The test steps included adjusting the frequency of the fan through the motor frequency converter governor, adjusting the wind speed from the fan output to the inlet of the feed injector to 26 $m \cdot s^{-1}$, adjusting the rotational speed of the granule discharging shaft to 20, 40 and 60 $r \cdot min^{-1}$ with corresponding granule flow rates of 33.5, 67.0 and 101 $g \cdot s^{-1}$, respectively, opening the fan first and then turning on the speed control motor which was set in advance to control the speed of the granule discharge shaft (the granule discharge period was 30 s), and selecting eight rows as the test samples to be analyzed. The test was repeated five times.

3.5.1 Bench test results at 20 $r \cdot min^{-1}$ discharge shaft speed

When the mass flow rate of the transported particles is 33.5 $g \cdot s^{-1}$ (Fig. 11(a,b)), the system meets the requirements of the national standard for the consistency of the rows of discharge using optimal bellows parameters and a bellows length of 300–500 mm. With an increase in the length of the bellows, the coefficients of displacement consistency and consistency variation of the discharge rows decrease and then increase, before tending to stabilize when the length of the bellows is 400 mm. The coefficient of variation of displacement consistency of each row is 3.26% ± 0.46% for a bellows length of 500 mm, which is the optimum bellows parameter for the simulations.

A one-way analysis of variance (ANOVA) was performed using SPSS to determine the effect of bellows length on the coefficient of variation under this speed condition.

The significance level of a 600-mm bellows length is lower than 0.05 in comparison with other bellows lengths when the mass flow rate of transported particles is 33.5 $g \cdot s^{-1}$ (Fig. 11(c)), indicating that the difference between these groups is significant, whereas the difference between the other groups is

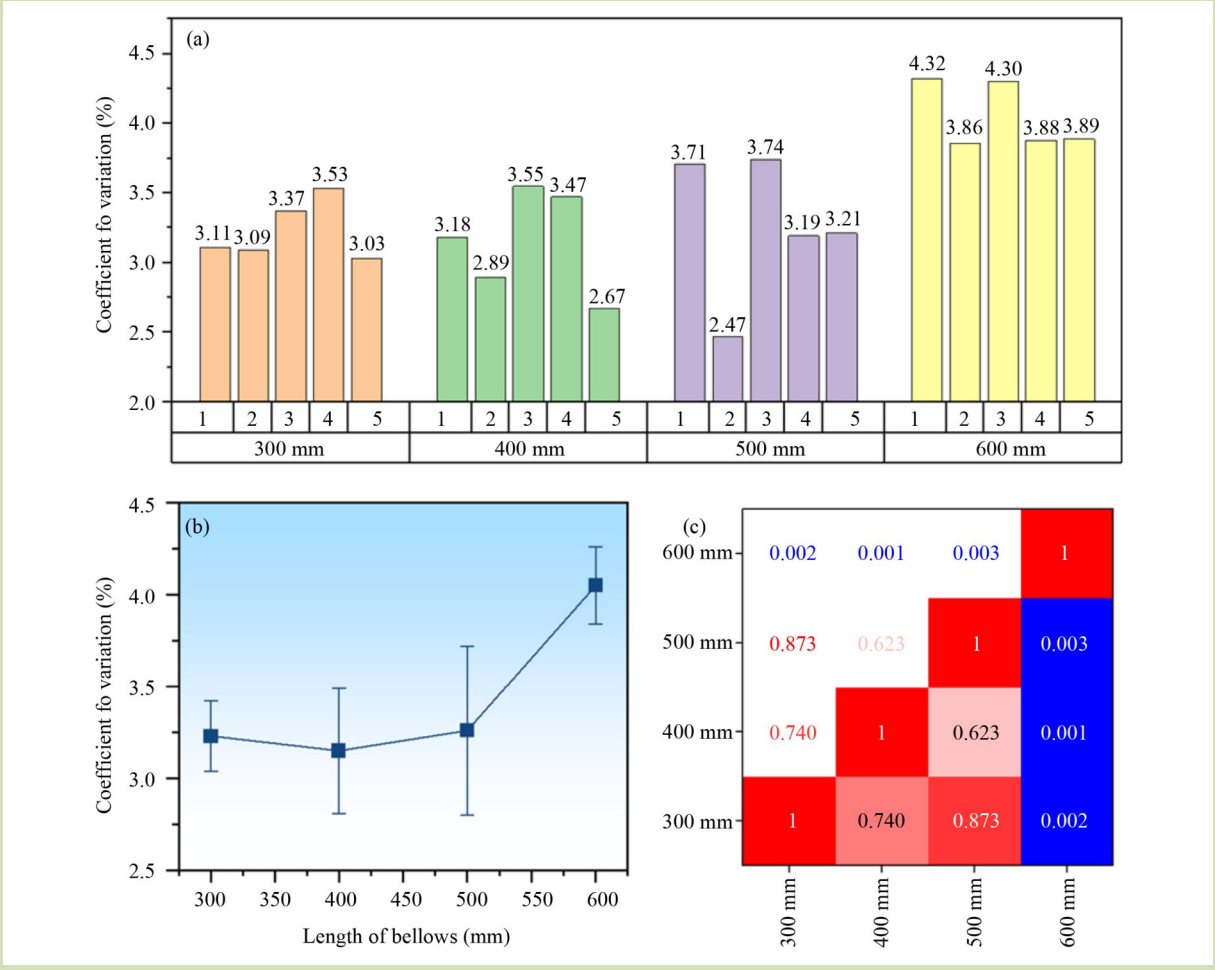

Fig. 11 Effect of different rotational speeds on seed distribution in bellows. (a) Measurement data of the consistency of the discharge volume of each row when the rotational speed of the granulation shaft is 20 r·min^{-1}, (b) influence of folded tube on displacement consistency when the rotation speed of the seed shaft is 20 r·min^{-1}, (c) one-way analysis of variance results (bluer colors or smaller values indicate more significant differences).

not significant.

A bellows length in the interval of 300–500 mm was determined to be the optimal solution for this flow rate (Fig. 11(c)).

3.5.2 Bench test results at 40 r·min^{-1} discharge shaft speed

When the mass flow rate of transported particles is 67.0 g·s^{-1} (Fig. 12(a,b)), the system meets the requirement of consistency of each row of discharge using optimal bellows parameters and a bellows length in the interval of 300–600 mm. With an increase in the length of the bellows, the coefficient of displacement consistency and consistency variation of the discharge rows decrease and then increase, tending to stabilize for a bellows length in the interval of 400–500 mm. The coefficient of variation of displacement consistency of each row of the system is the lowest when the bellows length is 500 mm. The coefficient of variation of the displacement consistency of each row is 2.11% ± 0.54% for the optimal bellows simulation parameter, that is, a bellows length of 500 mm.

A one-way ANOVA was performed to determine the effect of bellows length on the coefficient of variation for consistency of

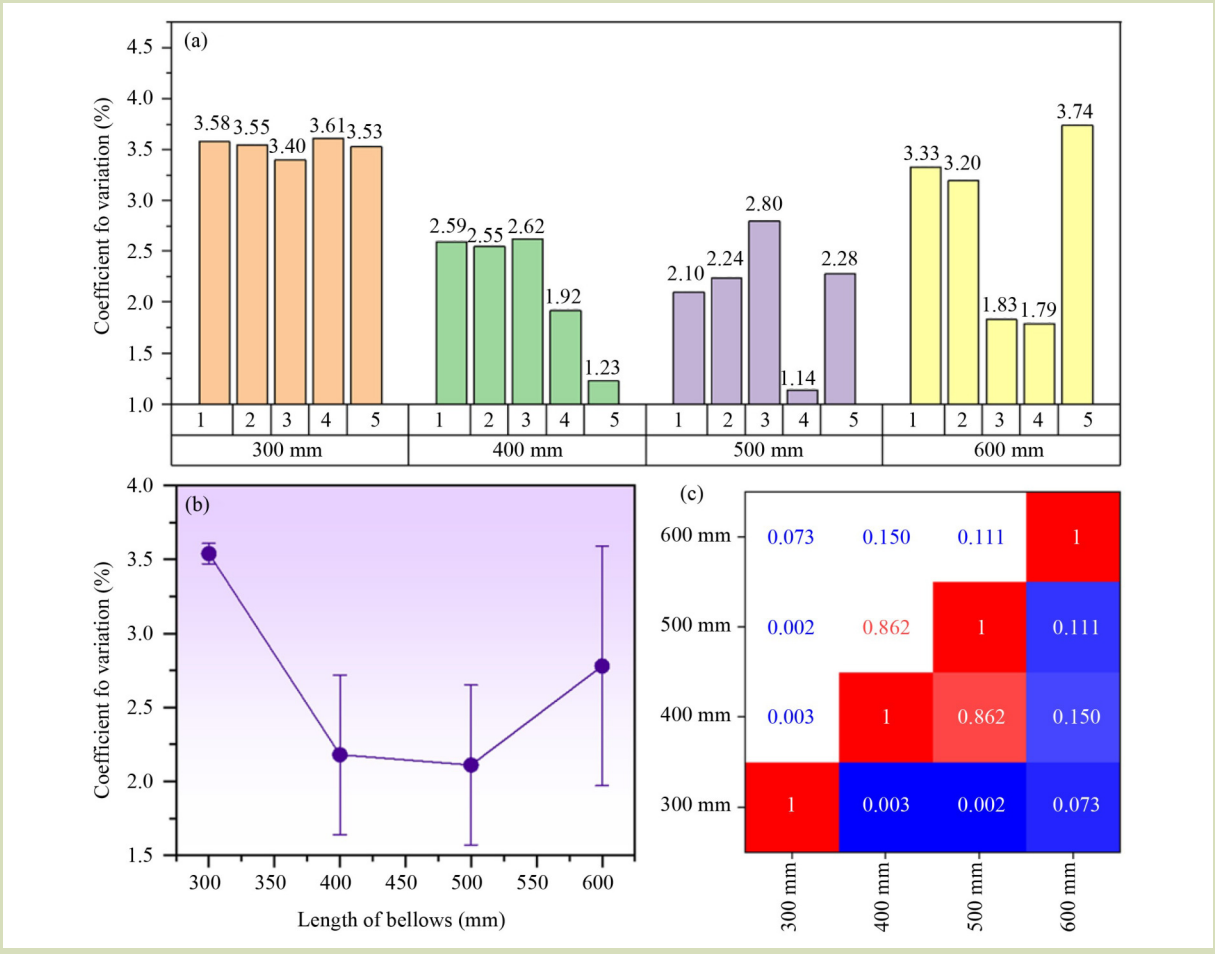

Fig. 12 Effect of different rotational speeds on seed distribution in bellows. (a) Measurement data of the consistency of the discharge volume of each row when the rotational speed of the granulation shaft is 40 r·min^{-1}, (b) influence of folded tube on displacement consistency when the rotation speed of the seed shaft is 40 r·min^{-1}, and (c) one-way analysis of variance results (bluer colors or smaller values indicate more significant differences).

displacement across rows under this speed condition.

At a mass flow rate of 67.0 g·s^{-1} of transported particles (Fig. 12(c)), the significance level for a bellows length of 300 mm versus lengths of 400–500 mm is lower than 0.05, which indicates that the difference between these groups is significant, whereas the difference between the other groups is not significant.

The bellows length in the interval of 400–500 mm was determined to be the optimal solution for this flow rate (Fig. 12(c)).

3.5.3 Bench test results at 60 r·min^{-1} discharge shaft speed

When the mass flow rate of transported particles is 101 g·s^{-1} (Fig. 13(a,b)), the system can meet the requirements of the national standard for the consistency of the rows of discharge using optimal bellows parameters and a bellows length in the interval of 300–600 mm. With an increase in the length of the bellows, the coefficient of consistency variation of the discharge rows shows a tendency to first increase, then stabilize, and then increase again. With an increase in the bellows length, the coefficient of variation of the displacement consistency of each row of the system is the lowest when the length of the bellows is 300 mm and tends to stabilize when the length of the bellows is in the interval of 400–500 mm. The coefficient of variation of

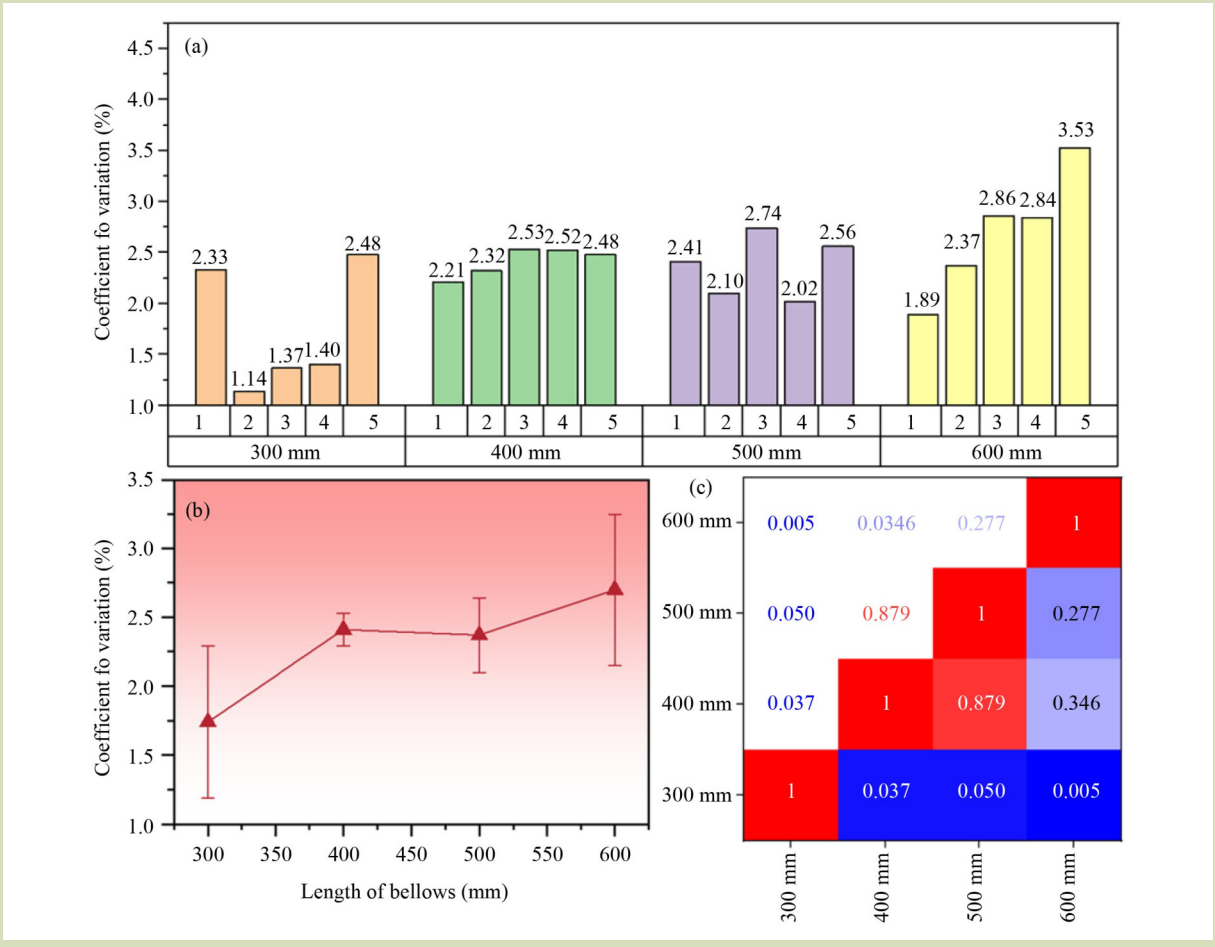

Fig. 13 Effect of different rotational speeds on seed distribution in bellows. (a) Measurement data of the consistency of the discharge volume of each row when the rotational speed of the granulation shaft is 60 r·min^{-1}, (b) influence of folded tube on displacement consistency when the rotation speed of the seed shaft is 60 r·min^{-1}, and (c) one-way analysis of variance results (bluer colors or smaller values indicate more significant differences).

displacement consistency of each row is 2.37 ± 0.27% for the optimum bellows simulation parameter of 500 mm bellows length.

A one-way ANOVA was performed to determine the effect of bellows length on the coefficient of variation for consistency of displacement across rows for this speed condition.

At a mass flow rate of 101 g·s^{-1} of transported particles (Fig. 13(c)), the significance level for a bellows length of 300 mm is lower than 0.05 with all other lengths indicating that the difference between these groups is significant, whereas the difference between the other groups is not significant.

The bellows length in the 300–600 mm interval was determined to be the optimal solution for this flow rate (Fig. 13(c)).

From the experimental data of the pneumatic distribution system under the three discharge conditions, a bellows length in the interval of 400–500 mm is the optimal solution that can simultaneously satisfy the requirements of the three displacements. In bellows simulations, the optimal solution was a bellows length of 500 mm when the mass flow rate of the transported particles was 33.5, 67.0 or 101 g·s^{-1}, with 3.26% ± 0.46%, 2.11% ± 0.54% and 2.37% ± 0.27%, as coefficients of consistency variation of the displacements of the rows of the

system, respectively, which are all within the optimal solution interval.

3.6 Discussion

Ideally, there should be few excess collisions inside the distributor and the vortex inside the distributor should not be sufficiently strong to affect the rice grains. A uniform particle-phase flow was fed into the inlet of the distributor, and the effect of the distributor was assumed to be perfect. Therefore, in the study of pneumatic distributor systems, the attention should be shifted from the distributor to the bellows or other key components to promote a uniform distribution of the particle phase in the cross-section of the plumbing tube.

In this study, the gas and particle phases were analyzed separately. Test 2 showed that the particle phase required a distance of more than 1 m to form a steady airflow in the vertical pipe. The particle-phase screenshot in Fig. 9 shows that a homogeneous particle phase can be formed even with no steady airflow in the bellows. Combined with theoretical analysis, more turbulent airflows were observed to contribute to the formation of a homogeneous particulate flow. Bench tests were conducted to verify this finding. Examples further supported this conclusion. For example, Test 1 found that the vertical pipe has the shortest stabilization stroke for the straight pipe, however, the particle-phase distribution in the straight pipe was not uniform. Analyses of the particle distribution in the straight tube and velocity distribution in the flow field suggest that a steady airflow contributes to particle stabilization but is not related to particle uniformity. Therefore, the coupled EDEM-Fluent approach can be used in the study of aerodynamic distribution systems, with attention focusing on the particle phase.

Bellows can effectively reduce the height of the air seeder compared with similar studies. A bellow length of 400–500 mm allows a uniform seed distribution, which is comparable to the height required for the wavy bellows of the peer study[11]. The total height (straight pipe + the bellow) is 700–800 mm. This is much lower than the 1.2 m required for a purely straight pipe[4]. Alternatively, the length of the straight pipe under the bellows can be increased if the seeder is required to be higher.

Some shortcomings of this study need to be noted. First, only the optimal combination of structural parameters was screened as dictated by practical requirements and the optimal parameters can be subsequently obtained by designing a Box-Behnken design optimization test method. Second, the movement of the seeds in the bellows can be observed using a high-speed camera. Third, the seedling emergence test or microscopic observation results can be used to compare rice damage under different bellows structures. Finally, the airflow velocity can affect particle uniformity and subsequent studies can experimentally obtain the minimum feasible airflow velocity under different sowing volumes to achieve higher energy utilization efficiency.

4 Conclusions

The right-angle pipe structure in the pneumatic distribution row seed-conveying system was fully considered in this study and the bellows were optimized using the coupled Fluent-EDEM method. The main conclusions are as follows.

Based on the results of this study, three principles can be summarized regarding the piping design of a pneumatic seed-discharge system: (1) horizontal pipes are designed as straight pipes to avoid pressure loss and shorten the airflow stabilization stroke of the vertical pipe; (2) the initial section of the vertical pipe is set as a straight pipe to avoid clogging of the particles at the 90° bend; and (3) an optimum length of the bellows in the range of 400–500 mm can guide the installation of pneumatic conveying pipes for a wide range of seeding machine models.

For the optimization of parameters, the primary and secondary factors affecting the dispersion effect of rice were identified, and the following parameters were optimized (corrugated circle radius of 8 mm, bellows length of 500 mm, corrugation pitch of 40 mm and corrugation length of 16 mm) to achieve an optimized coefficient of variation of 3.46% for the distribution of particles in the plumbing tube.

Experimental verification was conducted for system adaptability under a variety of particle mass flow rates (33.5, 67.0 and 101 $g{\cdot}s^{-1}$). The bellows length was the optimal solution in the interval of 400–500 mm, and the system consistency coefficients of variation of the rows of displacements met the requirements, thereby verifying the applicability and reliability of the design.

Acknowledgements

This work was funded by the National Key R&D Program of China (2022YFD2300700).

Compliance with ethics guidelines

Chengsai Fan, Biao Cheng, Jiaxin Tan, Ruiyin He, Gaoming Xu, and Jingliu Zhang declare that they have no conflicts of interest or financial conflicts to disclose. This article does not contain any studies with human or animal subjects performed by any of the authors.

REFERENCES

1. Wang L, Liao Y T, Li M L, Ren N, Zheng X M, Wang M Z, Liao Q X. Motion characteristics of rapeseeds and wheat seeds within mixing components of air-assisted centralized metering device based on DEM-CFD. *Computers and Electronics in Agriculture*, 2024, **221**: 108986
2. Yatskul A, Lemiere J P, Cointault F. Influence of the divider head functioning conditions and geometry on the seed's distribution accuracy of the air-seeder. *Biosystems Engineering*, 2017, **161**: 120–134
3. Cheng B, He R Y, Xu Y, Zhang X Z. Simulation analysis and test of pneumatic distribution fertilizer discharge system. *Agronomy*, 2022, **12**(10): 2282
4. Hu H J, Zhou Z L, Wu W C, Yang W H, Li T, Chang C, Ren W J, Lei X L. Distribution characteristics and parameter optimisation of an air-assisted centralised seed-metering device for rapeseed using a CFD-DEM coupled simulation. *Biosystems Engineering*, 2021, **208**: 246–259
5. Liang F C, Yang T, Shi H T, Meng J, Zhu Y X. Experimental investigation on the variable proportional distribution of gas-liquid two-phase flow using a novel distributor. *Chemical Engineering Research & Design*, 2024, **208**: 611–625
6. Zhang F, Ding Y H, Low Z X, Jia L X, Zhou G Y, Liu Y F, Zhong Z X, Xing W H. Effects of flow distributor structures and particle-wall interaction on baghouse gas-solid flow. *Separation and Purification Technology*, 2024, **335**: 126140
7. Yuan W S, Ji C Y, Liu Z Y, Jin C Q, Feng Y G. Influencing factors of the distribution accuracy and the optimal parameters of a pneumatic fertilization distributor in a fertilizer applicator. *Agronomy*, 2022, **12**(9): 2222
8. Lu Y, Tong Z B, Glass D H, Easson W J, Ye M. Experimental and numerical study of particle velocity distribution in the vertical pipe after a 90° elbow. *Powder Technology*, 2017, **314**: 500–509
9. Wang C, Liu M, Yan J J. Flow irreversibility versus wear of elbow-reducer connection with gas-solid two-phase flow: a numerical study *via* CFD-DEM coupling method. *Powder Technology*, 2023, **428**: 118835
10. Xiao F, Luo M, Huang F Y, Zhou M M, An J C, Kuang S B, Yu A B. CFD–DEM investigation of gas-solid flow and wall erosion of *Vortex* elbows conveying coarse particles. *Powder Technology*, 2023, **424**: 118524
11. Zaidi A A. Study of particle inertia effects on drag force of finite sized particles in settling process. *Chemical Engineering Research & Design*, 2018, **132**: 714–728
12. Lei X L, Liao Y T, Liao Q X. Simulation of seed motion in seed feeding device with DEM-CFD coupling approach for rapeseed and wheat. *Computers and Electronics in Agriculture*, 2016, **131**: 29–39
13. Li Y, Liu D X, Cui B L, Lin Z, Zheng Y H, Ishnazarov O. Studying particle transport characteristics in centrifugal pumps under external vibration using CFD-DEM simulation. *Ocean Engineering*, 2024, **301**: 117538
14. Ma L C, Wei L B, Pei X Y, Zhu X S, Xu D R. CFD-DEM simulations of particle separation characteristic in centrifugal compounding force field. *Powder Technology*, 2019, **343**: 11–18
15. Ma H Q, Zhou L Y, Liu Z H, Chen M Y, Xia X H, Zhao Y Z. A review of recent development for the CFD-DEM investigations of non-spherical particles. *Powder Technology*, 2022, **412**: 117972
16. Liao C C, Hsiau S S, Chang P S. Bottom wall friction coefficients on the dynamic properties of sheared granular flows. *Powder Technology*, 2015, **270**(Part A): 348–357
17. Chen S, Fan Y P, Yan Z H, Wang W, Lu C X. CFD simulation of gas–solid two-phase flow and mixing in a FCC riser with feedstock injection. *Powder Technology*, 2016, **287**: 29–42
18. Yan Z H, Wang D D, Wu L N, Lu C X. Mixing effects of high-speed jets in gas-solid riser and downer reactors. *Particuology*, 2024, **92**: 196–209
19. Horabik J, Molenda M. Parameters and contact models for DEM simulations of agricultural granular materials: a review. *Biosystems Engineering*, 2016, **147**: 206–225
20. Zhang Q, Wang Y J, Li H, Gao J F, Ding Y G. Optimization of a

precision symmetric finger-clamping garlic seed-metering device. *Frontiers of Agricultural Science and Engineering*, 2024, **11**(4): 626–641

21. Yuan J B, Wu C Y, Li H, Qi X D, Xiao X X, Shi X X. Movement rules and screening characteristics of rice-threshed mixture separation through a cylinder sieve. *Computers and Electronics in Agriculture*, 2018, **154**: 320–329
22. Sun J F, Chen H M, Duan J L, Liu Z, Zhu Q C. Mechanical properties of the grooved-wheel drilling particles under multivariate interaction influenced based on 3D printing and EDEM simulation. *Computers and Electronics in Agriculture*, 2020, **172**: 105329
23. He S Y, Qian C, Jiang Y C, Qin W, Huang Z S, Huang D M, Wang Z M, Zang Y. Design and optimization of the seed feeding device with DEM-CFD coupling approach for rice and wheat. *Computers and Electronics in Agriculture*, 2024, **219**: 108814
24. Xing H, Cao X M, Zhong P, Wan Y K, Lin J J, Zang Y, Zhang G Z. DEM-CFD coupling simulation and optimisation of rice seed particles seeding a hill in double cavity pneumatic seed metering device. *Computers and Electronics in Agriculture*, 2024, **224**: 109075
25. General Administration of Quality Supervision, Inspection and Quarantine of the People's Republic of China, National Standardization Administration. GB/T 25418–2022: Rice Drect Seeder. Beijing: *General Administration of Quality Supervision, Inspection and Quarantine of the People's Republic of China, National Standardization Administration*, 2022. Available at National Standard Full Text Disclosure System website on February 18, 2025